Hybrid Quantum-Classical Eigensolver Without Variation or Parametric Gates

Pejman Jouzdani[1, *] and Stefan Bringuier[1]

[1]*General Atomics, San Diego, CA*

(Dated: August 27, 2020)

The use of near-term quantum devices that lack quantum error correction, for addressing quantum chemistry and physics problems, requires hybrid quantum-classical algorithms and techniques. Here we present a process for obtaining the eigenspectrum of electronic quantum systems. This is achieved by projecting the Hamiltonian of a quantum system onto a limited effective Hilbert space specified by a set of computational basis. From this projection an effective Hamiltonian is obtained. Furthermore, a process for preparing short depth quantum circuits to measure the corresponding diagonal and off-diagonal terms of the effective Hamiltonian is given, whereby quantum entanglement and ancilla qubits are used. The effective Hamiltonian is then diagonalized on a classical computer using numerical algorithms in order to obtain the eigenvalues. The use case of this approach is demonstrated for ground-sate and excited states of BeH_2 and LiH molecules, and the density of states, which agrees well with exact solutions.

I. INTRODUCTION

Quantum computers offer the ability to address problems in quantum many-body chemistry and physics by quantum simulation or in a hybrid quantum-classical approach. The latter method is considered the most promising approach for noisy-intermediate scale quantum (NISQ) devices [1]. The prospect and benefits of quantum algorithms, along with suitable hardware, is in overcoming the complexity of the wavefunction of a quantum system as it scales exponentially with system size [2]. Therefore developing techniques and algorithms for NISQ era devices that may prove to have some computational advantage themselves, or establish a path towards ideas and foundations that provide advantage for future error-corrected quantum devices, is a worthwhile pursuit.

The leading algorithms intended to be executed on NISQ devices, which aim to determine solutions to an electronic Hamiltonian, are variational in nature [3]. One specific algorithm is the variational quantum eigensolver (VQE), which has been tremendously successful in addressing chemistry and physics problems on quantum hardware and NISQ devices [4–12]. However, the restriction or challenge that exist with VQE is the need for prior insight with regard to selecting the trial quantum state, i.e., ansatz circuit. Furthermore, the classical optimization of the ansatz parameters may be a poorly converging problem [13, 14] and therefore limit the applicability of VQE for obtaining results accurate enough for chemical or physical interpretation. Finally, the realization of ansatz circuits that are motivated by domain knowledge, for example the unitary coupled cluster ansatz for chemistry problems [15], may not be directly applicable on NISQ hardware and therefore requires clever modification to obtain hardware efficient ansätze [6, 7, 16].

In this work we present a pragmatic hybrid quantum-classical approach for calculating the eigenspectrum of a quantum system within an effective model. Firstly, an effective Hamiltonian is obtained through measurement of short-depth quantum circuits. The effective Hamiltonian is essentially the projection of the quantum system Hamiltonian onto a limited set of computational basis. The basis is prepared to ensure the dimensions of the corresponding matrix does not grow exponentially with the system size. In order to evaluate the matrix elements of the effective Hamiltonian, suitable non-parametric quantum circuits are specified. The quantum circuits are designed, executed, and measured. From the result of the measurements the diagonal and off-diagonal terms of the effective Hamiltonian matrix are obtained. On the classical side, the effective Hamiltonian matrix, with suitable dimensions, is diagonalized numerically using a classical computer. Additionally, we use indirect measurement rather than direct measurement [17].

The paper is organized in the following: A short background is presented in section II. In section III the steps taken in our hybrid quantum-classical approach are explained in detail. In section IV we demonstrate the application of this hybrid approach on simple chemical molecules BeH_2 and LiH.

II. BACKGROUND

Consider a quantum many-body system of electrons with the second quantized Hamiltonian:

$$\hat{H} = \sum_{ij} \kappa_{ij} a_i^\dagger a_j + \sum_{ijkl} v_{ijkl} a_i^\dagger a_j^\dagger a_k a_l. \qquad (1)$$

$a_i^\dagger$ and a_i are the creation and annihilation operators, respectively. The anticommutator for the creation and annihilation are given by: $a_i a_j^\dagger + a_j^\dagger a_i = \delta_{ij}$ and $a_i a_j + a_j a_i = a_i^\dagger a_j^\dagger + a_j^\dagger a_i^\dagger = 0$. These rules enforce the non-abelian group statistics for fermions, that is, under exchange of two fermions the wave-function yields a minus sign.

The indices in Eq. (1) refer to single-electron states.

The coefficients κ_{ij} and v_{ijkl} are the matrix integrals

$$\kappa_{ij} = \langle i | \hat{K}_1 | j \rangle \qquad (2)$$

and

$$v_{ijkl} = \langle ij | \hat{V}_{12} | kl \rangle, \qquad (3)$$

where $\hat{K}_1$ and $\hat{V}_{12}$ operators correspond to one- and two-body interactions respectively. Since $\hat{K}_1$ and $\hat{V}_{12}$ can depend on other parameters such as the distance between nuclei, the Hamiltonian in Eq. (1) represents a class of problems. However, this class of problems has the common property that the number of fermions is a conserved value. Strictly speaking, the terms in the Hamiltonian act on fixed-particle-number Hilbert spaces, $\mathcal{H}_{N_F}$, that have the correct fermionic antisymmetry with N_F denoting the number of electrons. In this paper we consider this class of electronic systems where the Hamiltonian is assumed to be in the form of Eq. (1). The coefficients expressed in Eqs. (2–3) can be obtained using software packages developed for quantum chemistry calculations that perform efficient numerical integration [18].

A. Mapping to qubits & computational basis

The Hamiltonian as written in Eq. (1) can be expressed in the form of qubit operations (i.e., pauli matrices). This requires a transformation that preserves the anticommutation of the annihilation and creation operators. One transformation that satisfies this criteria, and is based on the physics of spin-lattice models, is the Jordan-Wigner (JW) transformation [19]. The JW-transformed Hamiltonian takes the form

$$\hat{H} = \sum_s \lambda_s \hat{h}_s, \qquad (4)$$

in which λ_s's are scalar and a *Pauli string* operator $\hat{h}_s$ is defined as

$$\hat{h}_s = \hat{O}_1^s \otimes \cdots \otimes \hat{O}_N^s. \qquad (5)$$

$\hat{O}_i^s \in \{\hat{I}, \hat{X}, \hat{Y}, \hat{Z}\}$ acts on the i-th qubit, $\{\hat{X}, \hat{Y}, \hat{Z}\}$ are the three Pauli matrices [20] and $\hat{I}$ is the identity matrix with the number of qubits denoted as N.

If the number of $\hat{I}$ operators in the tensor product of $\hat{h}_s$ is $N-k$, we call $\hat{h}_s$ a k-local Pauli string operator. Upon the JW transformation of the Hamiltonian, the Fock basis second quantization representation is a one-to-one correspondence with the computational basis of the qubits [21]. Thus, a computational basis of

$$|\mathbf{n}\rangle = |n_0, n_1, \ldots, n_N\rangle, \qquad (6)$$

with N qubits, where $n_i \in \{0, 1\}$, is equivalent to a an antisymmetric Fock basis.

Within the finite, but exponentially large, Hilbert space spanned by 2^N computational basis set, an effective matrix representation of the Hamiltonian may be possible, specifically, if one can efficiently evaluate the matrix elements $\langle \mathbf{n}' | \hat{H} | \mathbf{n} \rangle$ for an arbitrary computational basis $|\mathbf{n}\rangle$ and $|\mathbf{n}'\rangle$. Furthermore, assuming that the dimensions of the resulting effective matrix are relatively small, the matrix can be diagonalized on a classical computer, where its eigenvalues approximate the spectrum of the original Hamiltonian.

In this paper we show how to evaluate a matrix element $\langle \mathbf{n}' | \hat{H} | \mathbf{n} \rangle$ for arbitrary computational basis $|\mathbf{n}\rangle$ and $|\mathbf{n}'\rangle$, using a quantum circuit that has a circuit depth $\mathcal{O}(N)$. We do so by using ancilla qubits, and thus $N+1$ physical resources are needed. Optionally, the measurement of a Pauli string can be performed indirectly, which increases the number of qubits to $N+2$. In addition, we discuss how to choose an effective subspace for a given electronic Hamiltonian, with a dimension N_s, based on physical motivations (see sec. III C). The condition $N_s << 2^N$ makes it possible to diagonalize the Hamiltonian on a classical computer. In sec. IV, we numerically demonstrate this method for simple quantum chemistry systems, focusing on ground-state energy and the density of state calculations of the low-energy spectrum.

III. CONSTRUCTING AN EFFECTIVE MATRIX REPRESENTATION FOR A HAMILTONIAN BY QUBIT MEASUREMENT

A. Effective Hamiltonian and circuit representation

We first consider a Hamiltonian $\hat{H}$ that is expressed in terms of Pauli strings as in Eq. (4). Additionally, a subspace with N_s corresponding computational bases $\mathcal{S} = \{|\mathbf{n}\rangle\}$, is considered such that $N_s << 2^N$. Let us define the *effective Hamiltonian* matrix as the projection of $\hat{H}$ onto this subspace; that is

$$\hat{H}_{eff} = \sum_{\mathbf{n}, \mathbf{n}' \in \mathcal{S}} \langle \mathbf{n} | \hat{H} | \mathbf{n}' \rangle \ |\mathbf{n}\rangle \langle \mathbf{n}' |. \qquad (7)$$

The next step is to define a simple quantum circuit that utilizes one ancillary qubit to measure $\langle \mathbf{n} | \hat{H} | \mathbf{n}' \rangle$ matrix element.

The dimension of $\hat{H}_{eff}$ depends on the choice of the subspace in $\mathcal{S}$. The choice of the subspace, intuitively, depends on the physics of the problem. However, the focus of this paper is towards quantum chemistry problems, which are a primary application for NISQ devices. For this class of Hamiltonians there is a systematic way to select the appropriate subspace. This is discussed in Sec. III C.

The evaluation of diagonal terms in $\hat{H}_{eff}$, e.g., $\langle \mathbf{n} | \hat{H} | \mathbf{n} \rangle$, is trivially performed by preparing N qubits as a bit string of $|\mathbf{n}\rangle \equiv (n_0, \ldots, n_N)$ and measuring $\hat{H}$. The measurement of the total Hamiltonian is obtained through the measurement of every individual Pauli string, $\hat{h}_s$, in Eq. (5). The diagonal terms are then
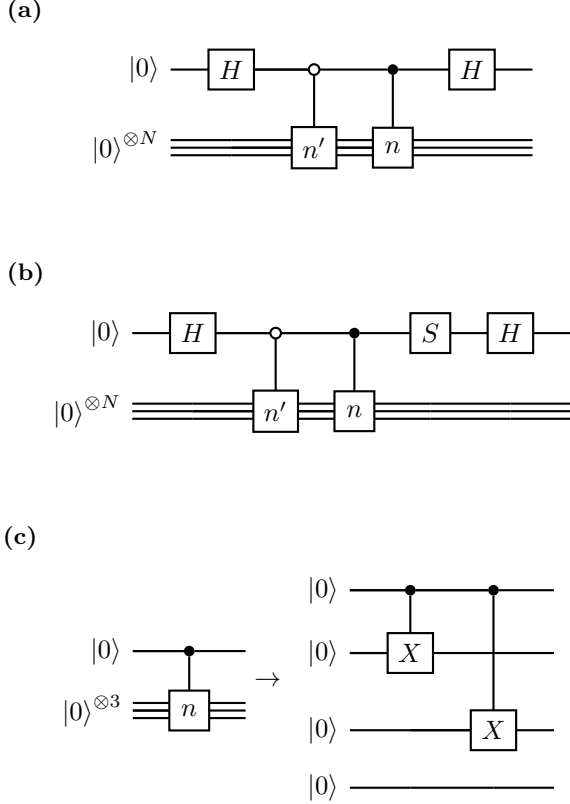
(a)

(b)

(c)

FIG. 1: Quantum circuits for measuring (a) the *real* and (b) *imaginary* parts of an off-diagonal element $\langle\mathbf{n}'|\,\hat{H}\,|\mathbf{n}\rangle$. (c) A controlled-$n$ gate represents a set of CNOT gates that prepares the qubits in the state $|n\rangle$. An example of controlled-n for $N=3$ and $|n\rangle = |011\rangle$ is shown.

given by

$$\langle\mathbf{n}|\,\hat{H}\,|\mathbf{n}\rangle = \sum_s \lambda_s \langle\mathbf{n}|\,\hat{h}_s\,|\mathbf{n}\rangle. \qquad (8)$$

The off-diagonal matrix elements, e.g., $\langle\mathbf{n}'|\,\hat{H}\,|\mathbf{n}\rangle$, which are generally complex numbers, can be evaluated using a single ancillary qubit. This can be seen by considering the quantum circuits as shown in Fig. 1. The two circuits shown in Fig. 1(a) and (b) are used to calculate the real and imaginary parts of the matrix element, respectively. In both circuits the $N+1$ qubits are initially prepared in $|\psi_{int}\rangle = |0\rangle \otimes |0\rangle^{\otimes N}$ state. The qubits are assumed to be enumerated linearly from 1 to $N+1$, where the $N+1$-th qubit is the control qubit.

After applying the first Hadamard gate on the ancillary qubit, from left to right as shown in the circuits in Fig. 1(a–b), the quantum state of all the qubits is

$$|\psi\rangle = \frac{1}{\sqrt{2}}\left[|0\rangle\,|0\rangle^{\otimes N} + |1\rangle\,|0\rangle^{\otimes N}\right], \qquad (9)$$

which, after a sequence of controlled-X gates, becomes

entangled as

$$|\psi\rangle = \frac{1}{\sqrt{2}}\left[|0\rangle\,|\mathbf{n}'\rangle + |1\rangle\,|\mathbf{n}\rangle\right]. \qquad (10)$$

Here control gates (controlled-n and controlled-n') flip N_F qubits (corresponding to the N_F occupied electronic states) and prepares the target qubits in the computational basis $|\mathbf{n}\rangle$ ($|\mathbf{n}'\rangle$), conditioned on the state of the control qubit is $|1\rangle$ ($|0\rangle$).

An example of a controlled-n gate that prepares target qubits in $|011\rangle$ state is shown in Fig. 1(c). In practice, this part of the circuit requires two-qubit gates (e.g., CNOT) and perhaps the need for full connectivity of qubits in order to operate on any two qubits. Full connectivity of qubits could potentially be realized with ion-trapped devices [22]. See sec. V for further discussion.

Depending on whether the *real part* or the *imaginary part* is calculated, the last gates acting on the control qubit changes. With regard to the *real part*, after applying the last Hadamard gate on the control qubit in Fig. 1(a), the quantum state is

$$|\psi\rangle = \frac{1}{2}|0\rangle\left[|\mathbf{n}'\rangle + |\mathbf{n}\rangle\right] + \frac{1}{2}|1\rangle\left[|\mathbf{n}'\rangle - |\mathbf{n}\rangle\right]. \qquad (11)$$

Using this prepared quantum state, one can measure

$$\hat{M}_0 = |0\rangle\langle 0| \otimes \hat{H}, \qquad (12)$$

at the end of the circuit and have

$$m_0 = \langle\psi|\left[|0\rangle\langle 0| \otimes \hat{H}\right]|\psi\rangle$$
$$= \frac{1}{2^2}\left(\langle\mathbf{n}|\,\hat{H}\,|\mathbf{n}\rangle + \langle\mathbf{n}'|\,\hat{H}\,|\mathbf{n}'\rangle + 2\mathbf{Re}\left[\langle\mathbf{n}|\,\hat{H}\,|\mathbf{n}'\rangle\right]\right). \qquad (13)$$

Thus, after substituting for the diagonal elements $\langle\mathbf{n}|\,\hat{H}\,|\mathbf{n}\rangle$ and $\langle\mathbf{n}'|\,\hat{H}\,|\mathbf{n}'\rangle$, using Eq. (8), one obtains the real part of the off-diagonal matrix element $\langle\mathbf{n}|\,\hat{H}\,|\mathbf{n}'\rangle$. The value m_0 in Eq. (13) is measured on a quantum device using the identity $|0\rangle\langle 0| = \frac{1}{2}(\hat{I} + \hat{Z})$, by

$$m_0 = \frac{1}{2}\langle\psi|\,\hat{I} \otimes \hat{H}\,|\psi\rangle + \frac{1}{2}\langle\psi|\,\hat{Z} \otimes \hat{H}\,|\psi\rangle$$
$$= \sum_s \frac{\lambda_s}{2}\langle\psi|\,\hat{I} \otimes \hat{h}_s\,|\psi\rangle + \frac{\lambda_s}{2}\langle\psi|\,\hat{Z} \otimes \hat{h}_s\,|\psi\rangle. \quad (14)$$

The *imaginary part* can be obtained in a similar fashion as done for the *real part* but with a slight modification to the circuit as shown in Fig. 1(b). The key addition is a phase-gate, S, before the execution of the last Hadamard gate on the control qubit. This yields the quantum state

$$|\psi\rangle = \frac{1}{2}|0\rangle\left[|\mathbf{n}'\rangle + i\,|\mathbf{n}\rangle\right] + \frac{1}{2}|1\rangle\left[|\mathbf{n}'\rangle - i\,|\mathbf{n}\rangle\right] \quad (15)$$

that now includes a phase factor i before $|\mathbf{n}\rangle$. After the last Hadamard gate in Fig. 1(b), and following the same steps, Eqs. (12)-(14), the imaginary part $\mathbf{Im}\left[\langle\mathbf{n}|\,\hat{H}\,|\mathbf{n}'\rangle\right]$ is obtained.

Our approach differs from the typical hybrid quantum-classical paradigm used in ground state chemistry electronic structure calculations in that the quantum hardware is used as a co-processor to measure these matrix elements. Therefore, no parameterized ansatz or variational optimization is required. In this approach the depth of the quantum circuit is significantly reduced, however, our method is based on the assumption that the dimensions of $\hat{H}_{eff}$ in Eq. (7) are reasonable enough such that it can be diagonalized using a classical numerical algorithms.

B. Implementing Measurements

As shown in Eq. (14) the expectation value of the Hamiltonian becomes the weighted sum of expectations for the set of Pauli string operators with respect to the output quantum state of the circuit. Since these operators are not in general commuting, one needs to set different quantum circuits for (up-to) every Pauli string in the Hamiltonian. Each circuit is then executed many times and every time the qubits are measured, the results are realized in different computational bases. The sampled realization provides a probability distribution and is used to estimate the expectation value of the Pauli string.

Generally, measurements are done either directly or indirectly. In the case of direct measurements, single-qubit rotations are applied to a subset of qubits at the end of the circuit. This subset is identified based on the locations in the tensor-product of the operator $\hat{h}_s$ that are not identity $\hat{I}$. This set of rotations essentially changes the computational bases in which the given operator $\hat{h}_s$ is diagonal. The direct measurement is commonly used in the experimental demonstration of quantum hardware and VQE [6].

The indirect measurement approach [23] requires a series of controlled gates that are applied to the N target qubits, using one ancillary control qubit. The indirect measurement method is used in iterative quantum phase estimation algorithms [24].

Although the two type of measurement approaches are theoretically equivalent [20], experimentally there are differences. The benefits and drawbacks of direct and indirect measurements are discussed for example in [17]. The main difference is the number of times the circuit is to be executed to achieve a desired precision ϵ, which is $\mathcal{O}(\frac{1}{\epsilon^2})$ and $\mathcal{O}(\frac{1}{\epsilon})$ for direct and indirect measurements respectively. The implementation of a general control-U gate in the indirect measurement is a challenging task [23]. However, for our purpose, where the U operator is a single Pauli string, the indirect measurement is more suitable.

In this paper we make use of the indirect measurement approach based on the circuit shown in Fig. 1. Consider the quantum circuit in Fig. 2. An additional control qubit is added to this circuit. The Pauli operators are applied on the k locations of $\hat{h}_s$ when the control is in state $|1\rangle$.

It is straightforward to follow the quantum state of the qubits until the end of the circuit. The final state of the circuit is then:

$$|\psi\rangle = \frac{1}{2} |00\rangle \left[|\mathbf{n'}\rangle + |\mathbf{n}\rangle + \hat{h} |\mathbf{n'}\rangle + \hat{h} |\mathbf{n}\rangle \right] + \dots .$$

(16)

Now, consider measuring $\hat{M} = |0\rangle\langle 0| \otimes |0\rangle\langle 0| \otimes \hat{I}$, at the end of the circuit. Using Eq. (16), and steps discussed in sec. III A, it is possible to obtain the real part of the off-diagonal matrix element $\langle \mathbf{n'}| \hat{h}_s |\mathbf{n}\rangle$. The imaginary part is determined in a the similar manner by inclusion of a phase gate as indicated in Fig. 1(b).

In this indirect measurement, the value of $\langle\psi| \hat{M} |\psi\rangle$ is obtained from the expectations $\langle\psi| \hat{Z}_{N+2} |\psi\rangle$, $\langle\psi| \hat{Z}_{N+1} |\psi\rangle$, and $\langle\psi| \langle \hat{Z}_{N+2} \otimes \hat{Z}_{N+1} |\psi\rangle$, similar to Eq. (14)
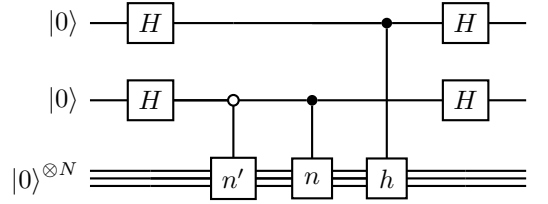

FIG. 2: Quantum circuit for indirect measurment of the *real* and *imaginary* parts of an arbitrary element $\langle \mathbf{n'}| \hat{h}_s |\mathbf{n}\rangle$, for a given Pauli string operator $\hat{h}_s$. Only controlled one-qubit gates are used. The first control qubit from the top is used for the measurement of the operator $\hat{h}_s$. The second control is to prepare the quantum state of the target qubits.

Finally, using the state preparation and measurements outlined through secs. III A–III B, all the $N_s \times N_s$ matrix elements of the effective Hamiltonian in Eq. (7) can be evaluated, by repeating the execution of the quantum circuits as discussed in Figs. 1-2, for all the possible combinations of a chosen set of $\{|\mathbf{n}\rangle\}$ bases.

We make note, that the approach for evaluating the *real* and *imaginary* parts of a matrix element is similar to the interference method introduced in ref. [10], with the difference being that this approach uses an ancillary qubit in order to realize the interference.

C. Preparing the computational basis

The computational basis set $\mathcal{S} = \{|\mathbf{n}\rangle\}$ with $N_s << 2^N$, needs to be specified in practice. These bases serve as the row and columns of $\hat{H}_{eff}$ in Eq. (7). The process and motivation for how to choose this set should be based on the underlying nature and physics of the problem.

In theory, one established approach to approximate the ground state of quantum many-body systems is by mean-field theory [25]. Where the true ground state is

constructed by perturbing the reference mean-field quantum state. The quantum chemistry field has established theories and techniques for treating such problems. One particularly successful theory and numerical method is coupled cluster (CC), typically referred to as the gold-standard in computational quantum chemistry [26]. In CC one assumes a wavefunction ansatz

$$|\psi\rangle = e^{\hat{T}} |\mathbf{0}\rangle, \qquad (17)$$

for the ground state. Here $|\mathbf{0}\rangle$ is a reference quantum state (e.g., Hartree-Fock) and is considered to be anti-symmetric under exchange of two fermions. The operator $\hat{T} = \hat{T}_1 + \hat{T}_2 + \cdots$ is a sum over different possible excitation operators above this reference state. Typically the set of excitation operators in $\hat{T}$ includes single and double terms (i.e., CCSD), which enables a series representation of the Taylor expansion of $e^{\hat{T}}$, but high-order terms can also be added. The coefficients for the excitation operators in $\hat{T}$ are determined by variational methods; that is by minimizing the expectation of the Hamiltonian with respect to the ansatz [26].

Since the exponential operator in the CC ansatz, Eq. (17), is non-unitary, it cannot be directly implemented on gate-based quantum computers, where gates correspond to unitary operators. Thus, a unitary version of the CC ansatz has been introduced and is known as Unitary Coupled Cluster (UCC) [15, 27]. Ideally, the implementation of UCC ansatz should be constructed such that the number of gates is minimized so that the circuit depth does not exhaust the current coherence times of NISQ devices. As a result of the this concern, hardware efficient anstaz have been proposed [6] as a substitute.

In this work, we consider a simplified ansatz for the ground state as:

$$\begin{aligned}
|\psi\rangle = {} & c_0 |\mathbf{0}\rangle \\
& + \sum_{i\nu} c_{i\nu} a_i^\dagger a_\nu |\mathbf{0}\rangle \\
& + \sum_{ij\nu\beta} c_{ij\nu\beta} a_i^\dagger a_j^\dagger a_\nu a_\beta |\mathbf{0}\rangle \\
& + \cdots, \qquad (18)
\end{aligned}$$

where $i, j, \ldots$ refer to the unoccupied levels, and $\nu, \beta, \ldots$, refer to occupied levels with respect to single (S), double (D), and higher order excitation operators. The ansatz in Eq. (18) implies that the true many-body ground state is a superposition of the reference state $|\mathbf{0}\rangle$ and all possible $S \{a_i^\dagger a_\nu |\mathbf{0}\rangle\}$, $D \{a_i^\dagger a_j^\dagger a_\nu a_\beta |\mathbf{0}\rangle\}$, up-to $\hat{T}_n |\mathbf{0}\rangle$ excitations, where n in $\hat{T}_n$ is finite and independent of N.

In particular, assuming that it is possible to truncate the series at some low-excitation level such as the D or triples (T), the number of eigen-states in the expansion of the above ansatz remains a polynomial function in N.

Taking the ansatz in Eq. (18), we specify the set $\mathcal{S}$ in the following way. (1) Pick a computational basis as the reference quantum state, that is $|\mathbf{0}\rangle = |\mathbf{n_{int}}\rangle$. (2) Identify computational bases corresponding to a finite number of excitations such as S and D. These are $N_s << 2^N$ bases and polynomial function in N.

In step (1), we identify the initial computational basis $|\mathbf{n_{int}}\rangle$ by minimizing the $\langle \mathbf{n_{int}} | \hat{H} | \mathbf{n_{int}} \rangle$, in which for example, a classical Monte Carlo process from spin lattice models [28] can be used. This computational basis is essentially the qubits' configuration that has the lowest energy expectation. Since this step is a classical one, it is performed effectively even for a large number of qubits.

In step (2), once the state $|\mathbf{n_{int}}\rangle$ is determined, one can rearrange the configuration of the qubits by swapping 1's and 0's within the state $|\mathbf{n_{int}}\rangle$. The swapping is done so that the configurations corresponding to S, D, up-to $\hat{T}_n$ are fully realized. The energy expectation corresponding to these configurations (the diagonal elements in the H_{eff}) are stored on a classical register. The final result is obtained among the set of configurations whereby N_s of are the lowest energies; these are the configurations that are selected. The above steps are demonstrated numerically which is discussed in the next section (see sec. IV).

IV. NUMERICAL DEMONSTRATION: LiH AND BeH$_2$

The application of the methodology discussed in sec. III is focused on BeH$_2$ and LiH molecules due to thier relatively small number of electrons and molecular orbital footprint. The number of electrons in BeH$_2$ and LiH is six and four, respectively. The single-electron molecular spin-orbitals in the second quantized Hamiltonian are constructed using the minimal atomic STO-3G basis set [2, 6]. For BeH$_2$ there are a total of 14 spin-orbital, and thus corresponds to 14 qubits; LiH contains 12 spin orbitals and hence 12 qubits. For the purpose of measuring the matrix elements of the effective Hamiltonian, Eq. (7), one additional ancillary qubit is required, as illustrated in the quantum circuits shown in Fig. 1. Therefore, the total number of qubits for the simulation of BeH$_2$ and LiH is 15 and 13, respectively.

To obtain the coefficients in the Hamiltonian of Eq. (1) — more specifically as defined in Eqs. (2) and (3) — we make use of the Psi4 quantum chemistry package [29]. The second quantized Hamiltonian is further transfomed onto a set of Pauli strings and their corresponding weights, Eq. (1), via JW transform using OpenFermion package [30].

In order to construct the potential energy surface for each inter-nuclear distance, R, the steps indicated in the previous paragraph are repeated. The distance R corresponds to the bond length between Be–H or Li–H in a given molecule; both LiH and BeH$_2$ are linear molecules. We note that these calculations are assuming the total Hamiltonian can be represented using the Born-Oppenheimer approximation, where the dynamics of the core nuclei are neglected. This is standard practice in quantum chemistry calculations [25] and thus at every distance R, the nuclear-nuclear repulsion energy is

treated classically and is added to the Hamiltonian as a constant.

For every distance R, a set of computational bases are chosen. This set includes the basis with the lowest energy expectation (the reference configuration) and computational bases that correspond to the low-order excitations (i.e., S, D, etc.) with respect to the reference configuration. In the case of BeH_2, we construct the effective Hamiltonian matrix by keeping the S, D, and T excitations, and thus the total number of computational bases for BeH_2 is $N_s = 1588$. The low dimension of the effective Hamiltonian matrix makes it possible to diagonalize the matrix on a classical computer using standard numerical techniques [31]. Thus, the lowest energies, including the ground-state energy, are obtained at every R. The results for this process are shown in Fig. 3.

Fig. 3(a) shows the ground-state energy as well as a few low-lying excited states for BeH_2 of the effective Hamiltonian. The exact energies are given by the dashed curves in Fig. 3(a). In Fig. 3(b) the difference between the exact and obtained ground-state energy is shown. An error within the hatched area indicates result that are within chemical accuracy. Chemical accuracy is typically identified as $\sim 5 \times 10^{-3}$ Hatrees. Figure 3(c) shows the same energy difference for all other excited-state energies. The same process is done for LiH where only S and D configurations are used. The total number of permutation of 4 fermions (495) is reduced to $N_s = 200$, and the results are shown in Fig. 4.

The total number of configurations can be approximated by the highest excitation considered. For n-electron excitation the number of configurations is $\binom{N_F}{n}\binom{N-N_F}{n} < N^{2n}$. Thus, the total number of configurations is less than $1 + \cdots + N^{2n} = \mathcal{O}(N^{2n})$ when $N \gg 1$. In the case BeH_2, where the highest excitation considered is T with $n = 3$, and therefore, an approximation to the number of configurations is N^6. The same assessment for LiH shows that N^4. Thus, for both cases the dimension of the effective Hamiltonian remains polynomial in N. Of course, this argument is valid as long as n can be assumed to be finite and independent of the size of the system N or the number of electrons N_F. Under these assumptions, the dimensions of the effective Hamiltonian stays polynomial as one replaces the minimal STO-3G with the extended atomic basis.

A. Density of States

Knowledge of density of states (DOS) can be important in analyzing the thermodynamic behaviour of a system at finite temperature and in the analysis of transition states important in chemical reactions [32]. One advantage of the proposed method in this paper is the insights provided into the low-energy spectrum of the quantum system, more precisely, the degeneracy of the energy levels. In Fig. 5 the unnormalized DOS of the LiH obtained via the effective Hamiltonian is compared with the exact
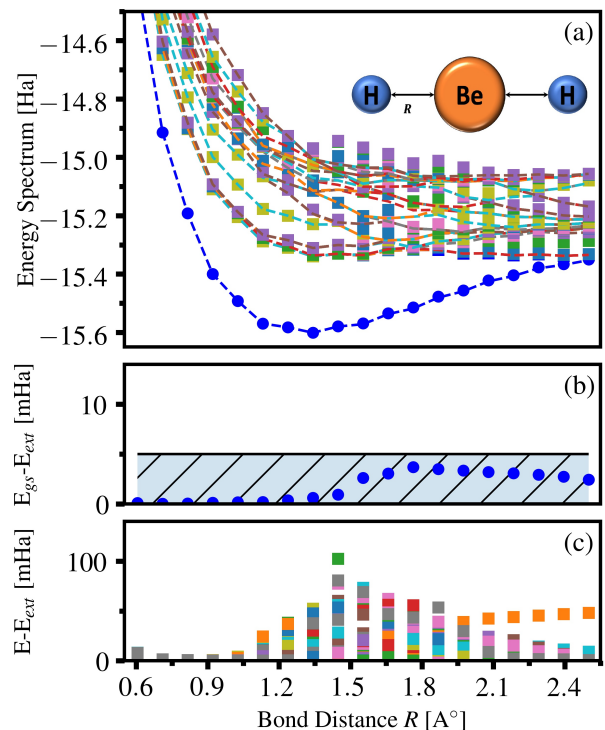

FIG. 3: (a) The calculated binding curve of BeH_2 for the ground state and several excited states demonstrating the application of the method described in this work. (b) The difference between the ground state energies obtained from diagonalization of the exact and the effective Hamiltonian along with the chemical accuracy line, and (c) is energy difference for the obtained excited state spectra within the effective model.

density, which shows qualitatively good agreement.

V. DISCUSSION AND SUMMARY

Recently an abundance of Variational Quantum Algorithms (VQA) have been introduced to solve electronic quantum many-body problems on NISQ devices [3–5, 8–11, 27]. These VQA proposals mostly rely on optimization of parametric circuits. In this paper we demonstrate for quantum chemistry problems that an alternative approach exists that does not require an optimization procedure and parametric ansatz. In this approach the quantum hardware is used only to prepare a many-body quantum state and to efficiently measure the expectation value of certain target observables with respect to this quantum state. From the output measurements, one can construct what we refer to as an effective Hamiltonian matrix, $\hat{H}_{eff}$. Upon diagonalization of $\hat{H}_{eff}$ using classical eigendecomposition numerical methods one obtains the ground state and low-lying excited states of the system.
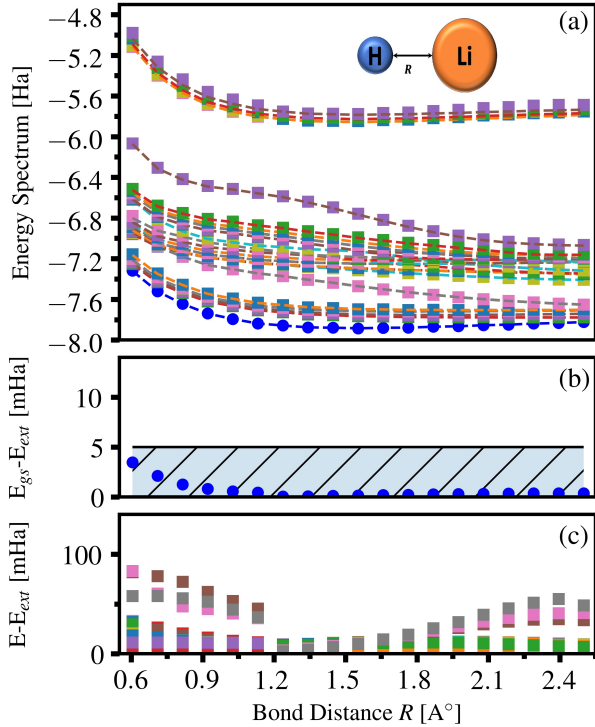
FIG. 4: Similar result as shown in Fig. 3 but for LiH.
(a) Shows ground state and excited states and (b-c)
indicate energy differences compared to exact
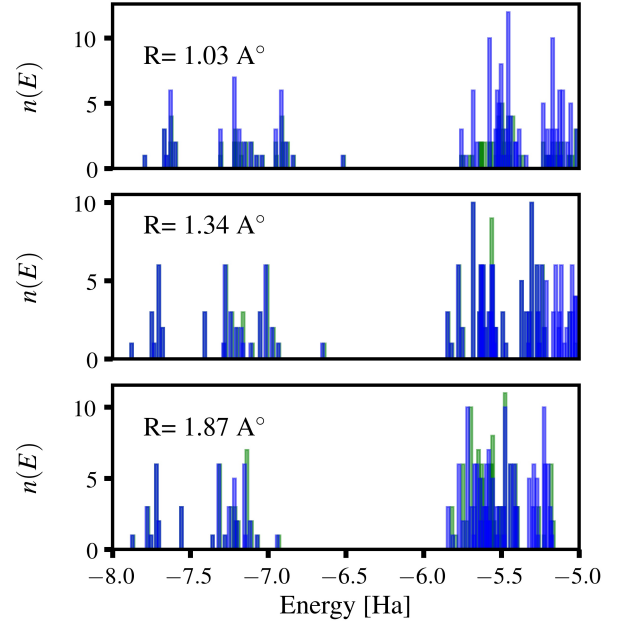diagonalization.

FIG. 5: The unnormalizaed density of states for LiH at
different binding distances. The blue fill indicates the
exact and the green fill indicates simulated

The approach introduced in this paper is particularly
suitable for NISQ devices where short quantum circuit
depth is essential due to lack of error-correction protocols
on these devices. An additional important aspect of this
approach is that it provides access to the low-lying energy
spectra of the system and not just the ground-state in
comparison with the original VQE process.

In the context of VQE and VQE-type algorithms, sev-
eral attempts have been made to extend the variational
approach to excited states [10, 11, 33–36]. Quantum sub-
space expansion [37, 38] for example constructs a set of
non-orthogonal bases out of an optimized ansatz, and
performs post-processing to obtain excited states. De-
flation techniques as described in ref. [11], constructs
a pseudo-Hamiltonian in which the ground-state is ex-
cluded and orthogonality is enforced through regulariza-
tion. Successful examples are introduced for some low-
lying excited states of LiH [8]. In all these previous works,
optimization of a parametric ansatz is required therefore
necessitates an enormous number of quantum circuit ex-
ecutions and sampling.

The approach introduced in this paper is similar to
multistate contracted VQE (MC-VQE) in ref. [10]. The
main difference is the application of VQE: MC-VQE is
obviously a VQE-type algorithm, our approach is dis-
tinct in that it does not require a parametric circuit or
variational procedure for optimization. In addition our

method differs since it uses supporting quantum circuit
resources, that is ancilla qubits, in order to perform in-
terference and measurement which is different from the
quantum circuit in ref. [39] and its generalization in
ref. [10].

An extension of our approach to VQE type algorithm
is possible. This can be done by appending a set of para-
metric gates that act only on the target qubits to the
circuits in Fig. 1. Let us denote this part of the circuit
with $U(\theta)$, where θ stands for a set of parameters. Then,
it can be verified that, given θ, the final matrix element
obtained from the circuit after measurement (see Eq. (2)
for example) becomes $\langle \mathbf{n} | U^\dagger(\theta) \hat{H} U(\theta) | \mathbf{n}' \rangle$, compared to
$\langle \mathbf{n} | \hat{H} | \mathbf{n}' \rangle$. The appended parametric circuit $U(\theta)$ allows
one to project the Hamiltonian onto $\mathcal{S}(\theta) = \{U(\theta) | \mathbf{n} \rangle\}$,
for a given θ. This means the $N_s \times N_s$ effective Hamilto-
nian is now parametric and depends on the value(s) of θ.
The optimal parameter(s) are then obtained by minimiz-
ing the ground state energy of the effective Hamiltonian
matrix. The reference state $\{U(\theta) | \mathbf{n} \rangle\}$ can be regarded
as the contracted reference states introduced in ref. [10].

One possible limitation of the circuits shown in Fig. 1 is
the execution of two-qubit gates corresponding to control
operations over n-qubits (i.e., series of CNOT gates).
For NISQ devices with hardware-restricted qubit connec-
tivity this may require a number of SWAP gate opera-
tions and therefore can increase the circuit depth and
subsequent error rates [40, 41]. In essence, the imple-
mentation of the circuits described in this paper will
depend on the ability to limit circuit depth and associ-
ated error rates by NISQ hardware circuit optimization

(i.e., scheduling). However, significant improvements in qubit connectivity of various modalities (e.g., ion traps) [22, 42] or optimizing quantum circuits against decoherence [43, 44] may blunt this concern.

VI. ACKNOWLEDGEMENT

Disclaimer: A portion of this report was prepared as an account of work sponsored by an agency of the United States Government. Neither the United States Government nor any agency thereof, nor any of their employees, makes any warranty, express or implied, or assumes any legal liability or responsibility for the accuracy, completeness, or usefulness of any information, apparatus, product, or process disclosed, or represents that its use would not infringe privately owned rights. Reference herein to any specific commercial product, process, or service by trade name, trademark, manufacturer, or otherwise does not necessarily constitute or imply its endorsement, recommendation, or favoring by the United States Government or any agency thereof. The views and opinions of authors expressed herein do not necessarily state or reflect those of the United States Government or any agency thereof.

[1] J. Preskill, Quantum **2**, 79 (2018), ISSN 2521-327X, URL https://doi.org/10.22331/q-2018-08-06-79.
[2] S. McArdle, S. Endo, A. Aspuru-Guzik, S. C. Benjamin, and X. Yuan, Reviews of Modern Physics **92**, 015003 (2020).
[3] X. Yuan, S. Endo, Q. Zhao, Y. Li, and S. C. Benjamin, Quantum **3**, 191 (2019).
[4] A. Peruzzo, J. McClean, P. Shadbolt, M.-H. Yung, X.-Q. Zhou, P. J. Love, A. Aspuru-Guzik, and J. L. Obrien, Nature communications **5**, 4213 (2014).
[5] J. R. McClean, J. Romero, R. Babbush, and A. Aspuru-Guzik, New Journal of Physics **18** (2016), ISSN 13672630, 1509.04279.
[6] A. Kandala, A. Mezzacapo, K. Temme, M. Takita, M. Brink, J. M. Chow, and J. M. Gambetta, Nature **549**, 242 (2017).
[7] P. K. Barkoutsos, J. F. Gonthier, I. Sokolov, N. Moll, G. Salis, A. Fuhrer, M. Ganzhorn, D. J. Egger, M. Troyer, A. Mezzacapo, et al., Phys. Rev. A **98**, 022322 (2018), URL https://link.aps.org/doi/10.1103/PhysRevA.98.022322.
[8] T. Jones, S. Endo, S. McArdle, X. Yuan, and S. C. Benjamin, Phys. Rev. A **99**, 062304 (2019), URL https://link.aps.org/doi/10.1103/PhysRevA.99.062304.
[9] K. M. Nakanishi, K. Mitarai, and K. Fujii, Phys. Rev. Research **1**, 033062 (2019), URL https://link.aps.org/doi/10.1103/PhysRevResearch.1.033062.
[10] R. M. Parrish, E. G. Hohenstein, P. L. McMahon, and T. J. Martínez, Phys. Rev. Lett. **122**, 230401 (2019), URL https://link.aps.org/doi/10.1103/PhysRevLett.122.230401.
[11] O. Higgott, D. Wang, and S. Brierley, Quantum **3**, 156 (2019), ISSN 2521-327X, URL https://doi.org/10.22331/q-2019-07-01-156.
[12] P. Jouzdani, S. Bringuier, and M. Kostuk, *A method of determining excited-states for quantum computation* (2019), arXiv:1908.05238.
[13] J. R. McClean, S. Boixo, V. N. Smelyanskiy, R. Babbush, and H. Neven, Nature communications **9**, 1 (2018).
[14] R. M. Parrish, J. T. Iosue, A. Ozaeta, and P. L. McMahon, *A jacobi diagonalization and anderson acceleration algorithm for variational quantum algorithm parameter optimization* (2019), arXiv:1904.03206.
[15] J. Romero, R. Babbush, J. R. McClean, C. Hempel, P. Love, and A. Aspuru-Guzik, *Strategies for quantum computing molecular energies using the unitary coupled cluster ansatz* (2017), arXiv:1701.02691.
[16] Y. Herasymenko and T. E. O'Brien, *A diagrammatic approach to variational quantum ansatz construction* (2019), 1907.08157.
[17] K. Mitarai and K. Fujii, Phys. Rev. Research **1**, 013006 (2019), URL https://link.aps.org/doi/10.1103/PhysRevResearch.1.013006.
[18] S. Reine, T. Helgaker, and R. Lindh, Wiley Interdisciplinary Reviews: Computational Molecular Science **2**, 290 (2012).
[19] E. Fradkin, Physical review letters **63**, 322 (1989).
[20] M. A. Nielsen and I. Chuang, *Quantum computation and quantum information* (American Association of Physics Teachers, 2002).
[21] M. Steudtner and S. Wehner, Phys. Rev. A **99**, 022308 (2019), URL https://link.aps.org/doi/10.1103/PhysRevA.99.022308.
[22] K. Wright, K. M. Beck, S. Debnath, J. M. Amini, Y. Nam, N. Grzesiak, J.-S. Chen, N. C. Pisenti, M. Chmielewski, C. Collins, et al., Nature Communications **10** (2019), ISSN 2041-1723, URL http://dx.doi.org/10.1038/s41467-019-13534-2.
[23] E. Knill, G. Ortiz, and R. D. Somma, Phys. Rev. A **75**, 012328 (2007), URL https://link.aps.org/doi/10.1103/PhysRevA.75.012328.
[24] M. Dobšíček, G. Johansson, V. Shumeiko, and G. Wendin, Phys. Rev. A **76**, 030306 (2007), URL https://link.aps.org/doi/10.1103/PhysRevA.76.030306.
[25] F. Jensen, *Introduction to computational chemistry* (John wiley & sons, 2017).

[26] R. J. Bartlett and M. Musiał, Reviews of Modern Physics **79**, 291 (2007).

[27] D. Wecker, M. B. Hastings, and M. Troyer, Phys. Rev. A **92**, 042303 (2015), URL https://link.aps.org/doi/10.1103/PhysRevA.92.042303.

[28] W. Janke, *Monte Carlo Simulations of Spin Systems* (Springer Berlin Heidelberg, Berlin, Heidelberg, 1996), pp. 10–43, ISBN 978-3-642-85238-1, URL https://doi.org/10.1007/978-3-642-85238-1_3.

[29] R. M. Parrish, L. A. Burns, D. G. A. Smith, A. C. Simmonett, A. E. DePrince, E. G. Hohenstein, U. Bozkaya, A. Y. Sokolov, R. Di Remigio, R. M. Richard, et al., Journal of Chemical Theory and Computation **13**, 3185 (2017), URL https://doi.org/10.1021/acs.jctc.7b00174.

[30] J. R. McClean, K. J. Sung, I. D. Kivlichan, Y. Cao, C. Dai, E. S. Fried, C. Gidney, B. Gimby, P. Gokhale, T. Hner, et al., *Openfermion: The electronic structure package for quantum computers* (2017), 1710.07629.

[31] P. Virtanen, R. Gommers, T. E. Oliphant, M. Haberland, T. Reddy, D. Cournapeau, E. Burovski, P. Peterson, W. Weckesser, J. Bright, et al., Nature Methods (2020).

[32] D. G. Truhlar, B. C. Garrett, and S. J. Klippenstein, The Journal of physical chemistry **100**, 12771 (1996).

[33] J. Tilly, G. Jones, H. Chen, L. Wossnig, and E. Grant (2020), arXiv:2001.04941.

[34] R. Santagati, J. Wang, A. A. Gentile, S. Paesani, N. Wiebe, J. R. McClean, S. Morley-Short, P. J. Shadbolt, D. Bonneau, J. W. Silverstone, et al., Science Advances **4** (2018), https://advances.sciencemag.org/content/4/1/eaap9646.full.pdf.

[35] S. McArdle, T. Jones, S. Endo, Y. Li, S. C. Benjamin, and X. Yuan, npj Quantum Information **5** (2019), ISSN 2056-6387, URL http://dx.doi.org/10.1038/s41534-019-0187-2.

[36] R. D. Somma, *Quantum eigenvalue estimation via time series analysis* (2019), 1907.11748.

[37] J. R. McClean, M. E. Kimchi-Schwartz, J. Carter, and W. A. de Jong, Physical Review A **95** (2017), ISSN 2469-9934, URL http://dx.doi.org/10.1103/PhysRevA.95.042308.

[38] J. I. Colless, V. V. Ramasesh, D. Dahlen, M. S. Blok, M. E. Kimchi-Schwartz, J. R. McClean, J. Carter, W. A. de Jong, and I. Siddiqi, Phys. Rev. X **8**, 011021 (2018), URL https://link.aps.org/doi/10.1103/PhysRevX.8.011021.

[39] F. Diker, *Deterministic construction of arbitrary w states with quadratically increasing number of two-qubit gates* (2016), arXiv:1606.09290.

[40] D. Venturelli, M. Do, E. Rieffel, and J. Frank, Quantum Science and Technology **3**, 025004 (2018), URL https://doi.org/10.1088%2F2058-9565%2Faaa331.

[41] B. Nash, V. Gheorghiu, and M. Mosca, Quantum Science and Technology **5**, 025010 (2020), URL https://doi.org/10.1088%2F2058-9565%2Fab79b1.

[42] S. Hazra, K. V. Salunkhe, A. Bhattacharjee, G. Bothara, S. Kundu, T. Roy, M. P. Patankar, and R. Vijay, Applied Physics Letters **116**, 152601 (2020), https://doi.org/10.1063/1.5143440, URL https://doi.org/10.1063/1.5143440.

[43] Y. Zhang, H. Deng, Q. Li, H. Song, and L. Nie, in *2019 International Symposium on Theoretical Aspects of Software Engineering (TASE)* (IEEE, 2019), pp. 184–191.

[44] A. Holmes, M. R. Jokar, G. Pasandi, Y. Ding, M. Pedram, and F. T. Chong, arXiv preprint arXiv:2004.04794 (2020), 2004.04794.

[45] A. Kay (2019), URL https://royalholloway.figshare.com/articles/Quantikz/7000520.

[46] J. D. Hunter, Computing in Science & Engineering **9**, 90 (2007).